Jaumann-like Rasorber Offering Angular Stability with Wideband Absorption and Low Insertion Loss

Jaumann-like Rasorber Offering Angular Stability with Wideband Absorption and Low Insertion Loss

Callum J. Hodgkinson, Dimitris E. Anagnostou, Senior Member, IEEE, Symon K. Podilchak, Member, IEEE

***Abstract*—A Jaumann-like rasorber is examined which offers wideband absorption, angular stability, and polarisation insensitivity. The structure is defined by three layers with two resistive layers placed on top of a lossless layer. Also, all three layers use capacitors to ensure compactness for the metasurface rasorber. These features provide broad angular stability up to 55° while also maintaining low insertion losses of about 1 dB and only 0.6 dB for measured broadside incidence. The rasorber is also shown to work as a radome in the near-field of a planar antenna array.**

***Index Terms*—Radome, absorber, polarisation insensitivity.**

I. Introduction

THERE has recently been significant research devoted to antenna radomes realised using metasurfaces. Some applications include grating lobe mitigation [1], gain enhancement [2], and radar scattering reduction. One such low scattering structure is a rasorber (or radome absorber). This is a frequency-selective absorbing metasurface with a passband to offer practical antenna integration for radome scenarios.

The first rasorber design was reported in 2006 [3] but the name first appeared in 2014 [4]. Such structures are generally based on a classic Salisbury screen concept, in which a ground layer and a resistive sheet are spaced a quarter-wavelength apart. To create a passband, however, the layers (or sheets) of the rasorber are usually defined using frequency selective surfaces (FSSs). This signal transmission passband (for a back-end antenna system), can be between two absorption bands [4], below/above an absorption band [6], or, be defined by multiple transmission bands [7]. The benefit of a rasorber over more conventional FSS radomes, is the out-of-band absorbing functionality that the structure provides to reduce the back-end antenna scattering effects. Therefore, to enhance the radar scattering reduction over frequency, as examined in this letter, the absorption bands should be as wide as possible.

The proposed three-layered rasorber structure, which maximises its absorption BWs (see Figs. 1 and 2 inset), is achieved by stacking two resistive layers above a bottom lossless layer. This configuration means the proposed rasorber is more akin to that of a Jaumann absorber, where multiple resistive layers are placed above a metallic ground. A similar configuration to this classic architecture, yet also different, was chosen due to the absorption and angular stability benefits associated with Jaumann absorbers (when compared with a Salisbury screen). Another important consideration, when designing rasorbers, is to ensure that any design has minimal impact on the back-end antenna system or transceiver array. Therefore, any successful rasorber design must be as transparent as possible, i.e. have very small insertion losses, within its passband, to minimise any signal degradation or antenna interference.

Our proposed rasorber offers insertion loss values of about 0.6 dB (or less) for angles of incidence up to and including 40°, when measured within a calibrated anechoic chamber. In addition, due to the symmetry and layering of the developed unit cell, the design is polarisation insensitive and has wideband absorption. The downside of such passive designs is that they can only be used in conjunction with narrowband antennas. Therefore, for the use of wideband antennas, frequency reconfigurable structures like varactor-tunable FSSs [8] and rasorbers [9], [10] were designed, but these generally struggle to obtain the desirable low loss and polarisation insensitive features due to the required bias lines. See for example [10], where insertion loss values were reported to be 2.1 dB.

This letter reports the design and test of the proposed Jaumann-like rasorber which offers wideband absorption, low insertion losses, and polarisation insensitivity to incident TM and TE fields. Moreover, and as further outlined in Table I, our proposed rasorber provides a -10 dB reflection coefficient relative bandwidth (BW) of more than 130% as well as lower and upper 80% absorption BWs of about 104% and 33%, respectively, while also offering a narrow half-power bandwidth (HPBW) of 8% in the passband. As will also be shown in the paper, the fabricated rasorber was placed in the near-field (NF) of a six-element ultra-wideband (UWB) array, and measurements show negligible degradation for the far-field (FF) beam pattern as well as the realised gain at the rasorber passband. To the best knowledge of the authors, no similar passive rasorber has been reported in the open literature which offers similar broadband absorption, polarisation insensitivity, low loss, and wide-angle performance metrics.

II. Design Considerations and Simulations

The design of the proposed Jaumann-like rasorber consists of a lossless layer topped by two resistive layers, where each layer is separated by a gap of 12.2 mm filled with a low-loss and low-dielectric foam (Eccostock PP-4, $\epsilon_r = 1.06$). The resistive layers are defined by a Jerusalem cross surrounded by a square-ring structure and tapered dipole arms in the horizontal and vertical planes (see Fig. 1). This symmetry supports the noted polarisation insensitivity. The unit cell of the bottom metamaterial layer (also referred to as the lossless layer) is composed of a small square-ring slot bridged with the same capacitors as the upper resistive layers. A larger gap of 0.95mm is necessary between the inner and outer conductors of the bottom layer to ensure that the layers have the same resonant frequency. All of the PCB layers use a substrate of Rogers RO5008 (ϵ_r = 2.2) with a thickness of 0.508 mm.

TABLE I
COMPARISON OF THE OPTIMISED PARAMETERS (SIMULATED) FOR SEVERAL RECENTLY PUBLISHED PASSIVE RASORBER DESIGNS

Rasorber Design	Total Layers	Rasorber Thickness	-10 dB Reflection Coef. BW	Lower 80% Absorption BW	Upper 80% Absorption BW	Dual-Pol. Insensitivity	Angular Stability Range	Transmission HPBW
[4]	2	$0.11\lambda_L$	100%	32.8%	24.8%	No	Info Not Available	26.8%
[6]	2	$0.12\lambda_L$	97.5%	75.9%	No Band	No	45°	41.9%
[15]	2	$0.09\lambda_L$	114.1%	58.3%	27.6%	Yes	15°	31.3%
[16]	2	$0.10\lambda_L$	103.6%	Info Not Available	Info Not Available	No	Info Not Available	23.6%
[17]	2	$0.15\lambda_L$	68.2%	68.4%	No Band	No	0°	10.9%
[18]	2	$0.11\lambda_L$	97.1%	51.3%	40.85%	No	Info Not Available	13.5%
[20]	2	$0.11\lambda_L$	105.4%	66.7%	34.4%	Yes	30°	11.8%
Proposed	**3**	$0.12\lambda_L$	**135.8%**	**103.8%**	**33.37%**	**Yes**	**55°**	**8.3%**

Note: λ_L refers to the free-space wavelength at the lowest frequency for 80% absorption at broadside.

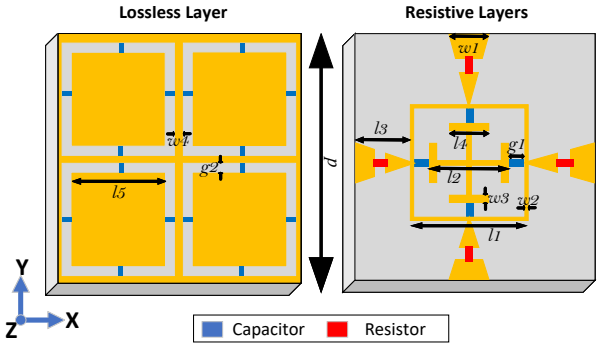

Fig. 1. Unit cell layouts for the multi-layer rasorber (see Table II details and stack-up, Fig. 2 inset). Lossy layers use 300Ω resistors and 0.2pF capacitors.

TABLE II
UNIT CELL DIMENSIONS WITHIN THE RASORBER LAYERS (SEE FIG. 1) WHERE λ REFERS TO THE FREE-SPACE WAVELENGTH AT RESONANCE

d	15mm (0.273λ)	$w1$	0.7mm (0.013λ)
$l1$	6.82mm (0.124λ)	$w2$	0.3mm (0.005λ)
$l2$	4.62mm (0.084λ)	$w3$	0.6mm (0.011λ)
$l3$	4.09mm (0.074λ)	$w4$	0.54mm (0.01λ)
$l4$	2.31mm (0.042λ)	$g1$	0.8mm (0.015λ)
$l5$	5.06mm (0.092λ)	$g2$	0.95mm (0.017λ)

For the unit cell design of the resistive layers, it was decided to use a printed Jerusalem cross. This is because such centre-cross elements generally provide greater angular stability when compared to other solid-interior implementations [5], as well as Jerulsaem crosses, in particular, having a low resonant frequency enabling compactness. This cross was then placed inside a square ring and lumped element capacitors were positioned between these shapes (see Fig. 1) to create a compact, sub-wavelength unit cell. Basically, with the use of the capacitors, our rasorber offers a small unit cell size and, therefore, a small periodicity of 15 mm (0.273λ at 5.46 GHz) and 7.5 mm for the lossless metamaterial layer (0.136λ). This small periodicity results in a high grating frequency [5] and should consequently create an angularly stable structure.

Another method to improve angular stability is to include multiple resistive layers but this can, however, also result in greater insertion loss [5]. It was therefore important to try and minimise these losses, and, given the motivations to attain low losses, our rasorber employs tapered dipole arms (which offer more wideband matching). Details are outlined in Fig. 1 and Table II. It should also be mentioned that the authors have reported initial findings of a reconfigurable rasorber in [9]. The newly optimised unit-cell reported in this letter, however, offers wider absorption BWs, lower insertion losses, and greater angular stability when compared to [9]. Also, the rasorber proposed in this letter has been manufactured and experimentally verified demonstrating these performance metrics, while also, its suitability for antenna array integration.

The rasorber was initially designed and simulated in CST Microwave Studio as a unit cell with infinite periodic boundary conditions. Fig. 2 shows the simulated transmission (S_{21}), and results indicate that the design supports transmission at 5.46 GHz with a small insertion loss of about 1 dB and for angular variations up to 55°. It can also be observed that the transmission coefficient offers a steep roll off away from this passband, with the transmission decreasing to less than -10 dB in a very short range both below and above the 5.46 GHz passband frequency. These results also imply that out-of-band absorption is achieved since the reflection coefficient in Fig. 3 is still reasonably matched both inside and outside the passband. Also, the reflections remains below -10 dB over an UWB frequency range and for various incident angles.

The equation $A = 1 - T - R$ was also used to calculate the absorption A of the structure, where T is the transmission coefficient (referring to $|S_{21}|^2$), and R is the reflection coefficient ($|S_{11}|^2$) [11]–[13]. Following this definition and by inspection of Fig. 4, it can be observed that the out-of-band absorption is very high and is greater than 80% between 2.0 to 4.4 GHz and 7.0 to 9.5 GHz for all angles.

Although the unit cell design is square and is clearly symmetric in both the x and y directions, simulation results were still needed to verify the polarisation insensitivity. The design was therefore examined for both TE and TM oriented incident waves defining the vertical and horizontal linearly polarised cases, respectively. These results are shown for off-broadside incidence in Fig. 5 and it can be observed that the transmission and reflection remains stable when the polarisation is varied, with no noticeable difference between the curves. Table III shows only a slight increase in insertion losses with increasing incident angle and no change in the resonant frequency. From these findings, the rasorber can be thought of as angularly stable and polarisation insensitive.

III. MEASUREMENTS AND DISCUSSIONS

For proof-of-concept of the proposed Jaumann-like rasorber, a finite 10×10 unit-cell structure measuring 150×150mm was manufactured and tested (see Fig. 6). MuRata 0.2pF

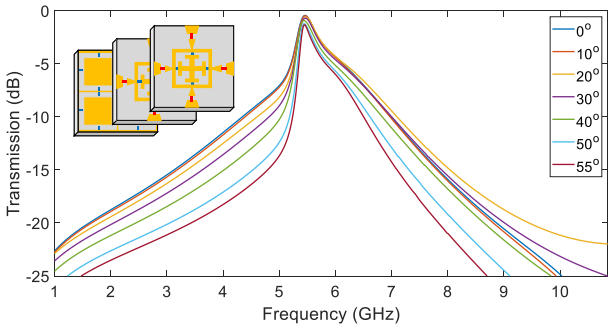

Fig. 2. The transmission for the rasorber considering an electric field linearly polarised in the vertical y-z plane (see Fig. 1, where the noted angle refers to tilt away from the z-axis towards the x-axis). Inset: three-layer unit cell.

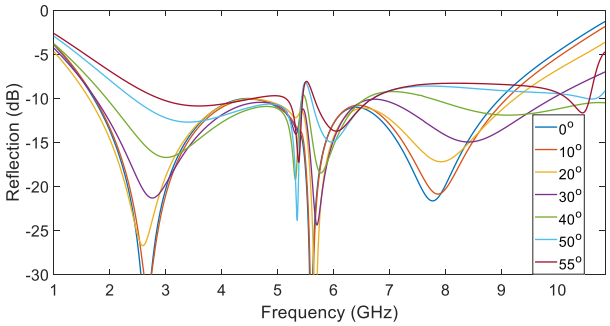

Fig. 3. The simulated reflection for the rasorber designed in CST.

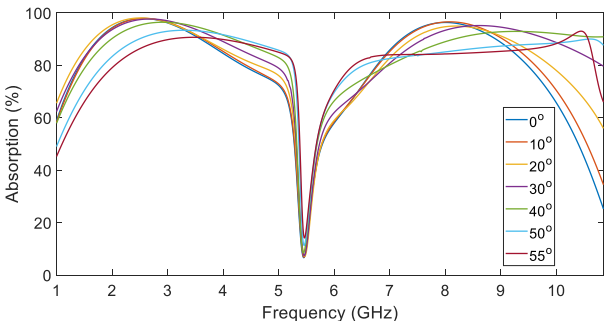

Fig. 4. The simulated absorption for the rasorber designed in CST.

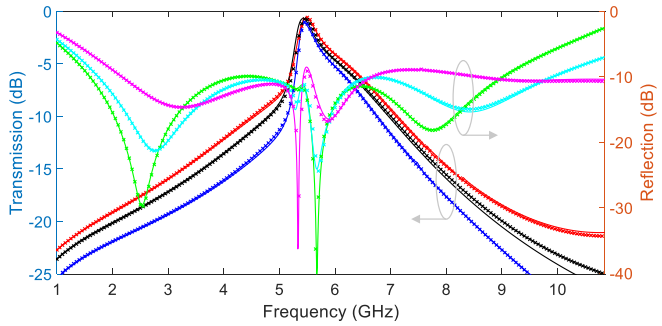

Fig. 5. Simulated transmission and reflection for both TE (y-axis) and TM (x-axis) incidence showing polarisation insensitivity. Transmission is denoted by red for 15°, black 30°, blue 45° and reflection is denoted by green 15°; cyan 30°; and magenta 45°. TE is shown by a solid line and TM with crosses.

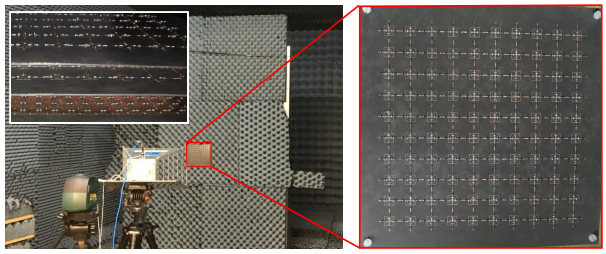

Fig. 6. Rasorber measurement photo (left); top view of the manufactured prototype (right); and side view of the multi-layer prototype (top left inset).

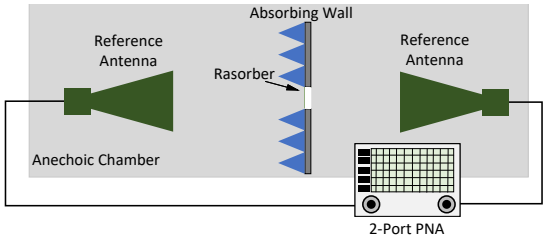

Fig. 7. Measurement setup devised to characterise the passive rasorber.

capacitors (GRM1555C1HR20WA01) and Panasonic 300Ω resistors (ERA2AEB301X) were selected. Fig. 7 illustrates the measurement setup where an absorbing wall was set in the FF between two reference horns (at a distance of 2.2m from each antenna), with a hole in the wall the size of the rasorber. To obtain the insertion loss, the transmission (S_{21}) was measured with and without the rasorber. Then the absorbing wall was rotated to study angular variation. The results in Fig. 8 and Table III suggest that simulations and measurements are in agreement. Also, the low structural losses reported and similarity to the simulations suggest that the manufactured design is working as intended, with minimal insertion loss whilst offering good angular stability.

The higher than expected transmission, for frequencies above the passband in Fig. 9, could be related to some manufacturing tolerances or minor bending of the layers due to the thin substrate employed (which were selected to help support low insertion losses). This bending concern could be mitigated by performing similar experiments but with a larger version of the rasorber. Since, for a larger design, these small imperfections should have less of an effect on performance. Also, the finite size of the structure might be related to the variations that can be observed at frequencies below the passband when the size becomes less than 2.5λ. Despite these minor deviations, there is a general agreement in the results, in that, the infinitely simulated structure offers similar functionality when compared to the finite rasorber. Given these findings, we felt that further practical investigations and prototyping, whilst considering a larger PCB structure, was not required for proof-of-concept realisation.

To measure the reflection coefficient (S_{11}) of the rasorber, the reference antennas were both placed on the same side of the absorbing wall, being almost co-located. Transmission, S_{21}, was then measured again for the following cases: (i) no rasorber; i.e. an open, (ii) with microwave absorber, (iii) and with a metal plate; i.e. a short. From these results the system could be calibrated for open and short representative reference

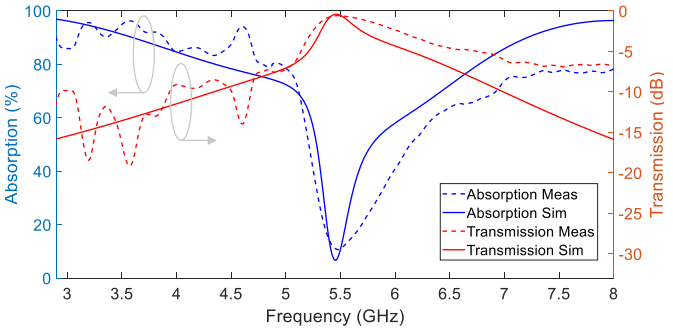

Fig. 8. The simulated and measured transmission and absorption for the rasorber considering broadside incidence.

TABLE III
ANGULAR STABILITY AND INSERTION LOSS AT RESONANCE (5.46 GHZ) FOR THE SIMULATED AND MEASURED RASORBER

Angle of Incidence	Simulated Loss	Measured Loss
0°	0.43 dB	0.60 dB
10°	0.47 dB	0.54 dB
20°	0.66 dB	0.53 dB
30°	0.70 dB	0.55 dB
40°	0.96 dB	0.58 dB

standards, and from this, the calibrated reflection coefficient was then determined. These reflection and transmission measurements were then used to calculate the absorption as shown in Fig. 10. The observed minor differences above and below the passband could be related to the practicalities mentioned earlier, and could also be linked to spurious diffraction or possible edge scattering effects from the finite structure (and this would have also cascaded to the calibrations). However, generally consistent result trends are observed for the simulations and the measurements. Therefore, it can be surmised that the rasorber offers wideband absorption, low loss, polarisation insensitivity, and 55° angular stability as per design.

To compare the results of the rasorber with other similar designs, Table I was compiled. It can be observed that our Jaumann-like design has a far-wider matching reflection BW when compared to other designs and this also results in much wider absorption bands. The design achieves these results without sacrificing polarisation, or angular stability (here, angular stability or the angular stable range, is defined where the rasorber still works as intended and with no change in resonance, and still with low reflections below -8 dB). The additional lossy layer does, however, cause a narrower half power bandwidth (HPBW) in the transmission band. This is not considered to be of great detriment to the overall antenna system, because, only the peak of the transmission frequency band and its angular stability is generally of interest for covered arrays and other rasorber scenarios.

Since the main purpose of the rasorber is to act as a practical radome, this had to be tested as well. Therefore, the beam pattern of a compact 6×1 UWB antipodal vivaldi array (see [14] for more details), was measured for uniform excitation in the rasorber passband at 5.46 GHz. In particular, the rasorber was placed in the radiative near-field (NF) of the array (at a distance of 0.25 m) and the FF beam pattern was measured using a standard reference horn. This was then

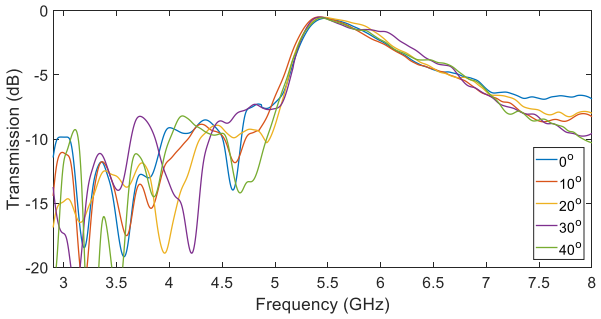

Fig. 9. The measured transmission (TE incidence) showing functionality. Stable angular stability is shown and with maximum transmission at 5.46GHz.

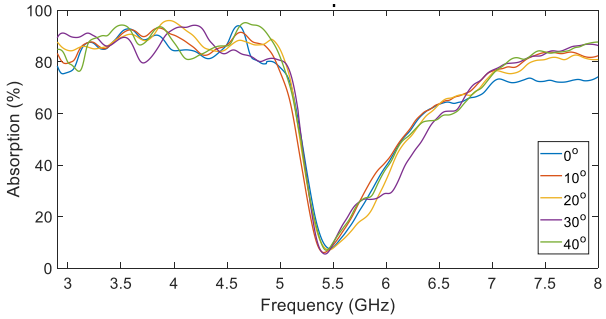

Fig. 10. The measured absorption for the rasorber (TE incidence). Dual-band absorption can be observed with values beyond 80%.

repeated without the rasorber. Patterns are shown in Fig. 11 and they demonstrate that the presence of the rasorber has little-to-no effect on the array, apart from a small drop in gain due to the minor transmission losses of the rasorber. For example, the measured realised gain without and with the rasorber was about 10 dBi and 9.4 dBi, respectively. These findings highlight the important functionality of the design, in that the proposed rasorber can act as an effective radome in the NF of an array without hampering its FF performance.

IV. CONCLUSION

This letter reports the design and measurement of a three-layered Jaumann-like rasorber. The results show that the additional resistive layer, and miniaturised unit cell, help provide 55° of angular stability as well as wideband absorption and a matching BW of more than 135%. The structure also offers dual-polarisation insensitivity and low insertion loss. Tests have also been completed to show that the rasorber can work in conjunction with an array to function as a practical radome.

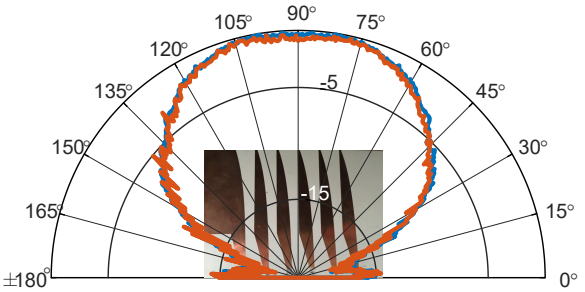

Fig. 11. Normalised patterns for a 6x1 UWB planar array (see [14] for more details on the array) measured at 5.46 GHz with (red) and without (blue) the presence of the rasorber which was placed in the NF of the array.

REFERENCES

[1] A. Monti et al., "Gradient Metasurface Dome for Phased arrays able Reducing the Grating Lobes within Single-side Scanning region," 2021 IEEE International Symposium on Antennas and Propagation and USNC-URSI Radio Science Meeting (APS/URSI), 2021, pp. 729-730.

[2] M. Chen, G. V. Eleftheriades and A. Epstein, "A Huygens' metasurface lens for enhancing the gain of frequency-scanned slotted waveguide antennas," 2018 United States National Committee of URSI National Radio Science Meeting (USNC-URSI NRSM), 2018, pp. 1-2.

[3] G. I. Kiani, A. R. Weily and K. P. Esselle, "A Novel Absorb/Transmit FSS for Secure Indoor Wireless Networks with Reduced Multipath Fading", IEEE Micr. Wire. Comp. Lett., vol. 16, no. 6, pp. 378-380, Jun. 2006.

[4] Y. Shang, Z. Shen and S. Xiao, "Frequency-Selective Rasorber Based on Square-Loop and Cross-Dipole Arrays," in IEEE Transactions on Antennas and Propagation, vol. 62, no. 11, pp. 5581-5589, Nov. 2014.

[5] B. Munk, Frequency Selective Surfaces. Hoboken: J.Wiley and Sons, 2000.

[6] M. Guo, Q. Chen, T. Bai, K. Wei and Y. Fu, "Wide Transmission Band Frequency-Selective Rasorber Based on Convoluted Resonator," in IEEE Ants. and Wire. Prop. Letters, vol. 19, no. 5, pp. 846-850, May 2020.

[7] G. Sen, S. Das and S. Ghosh, "Polarization-Insensitive Dual-Band Frequency Selective Rasorber based on Concentric SRRs," 2020 International Symposium on Antennas and Propagation (ISAP), 2021, pp. 263-264.

[8] M. Guo et al., "Analysis and design of a high-transmittance performance for varactor-tunable frequency-selective surface," in IEEE Transactions on Antennas and Propagation, vol. 69, no. 8, pp. 4623-4632, Aug. 2021.

[9] C. J. Hodgkinson, S. K. Podilchak and D. E. Anagnostou, "Jaumann-like Tuneable Rasorber with Enhanced Angular Stability and Polarisation Insensitivity," 2021 IEEE International Symposium on Antennas and Propagation and USNC-URSI Radio Science Meeting (APS/URSI), 2021, pp. 2034-2035.

[10] L. Wu, S. Zhong, J. Huang and T. Liu, "Broadband Frequency-Selective Rasorber With Varactor-Tunable Interabsorption Band Transmission Window," in IEEE Transactions on Antennas and Propagation, vol. 67, no. 9, pp. 6039-6050, Sept. 2019.

[11] Y. Shen, W. Li, Y. Pang, Z. Pei and S. Qu, "Double-layer resistive FSS structure for ultra-wideband microwave absorption," 2015 IEEE MTT-S International Microwave Workshop Series on Advanced Materials and Processes for RF and THz Applications (IMWS-AMP), 2015, pp. 1-3.

[12] Z. Lu, L. Ma, J. Tan, H. Wang, and X. Ding X, "Transparent multilayer graphene/polyethylene terephthalate structures with excellent microwave absorption and electromagnetic interference shielding performance," Nanoscale, Royal Society of Chemistry, vol. 8, no. 37, pp. 16684–16693, 2016.

[13] J. Ning, et al., "Ultra-broadband microwave absorption by ultra-thin metamaterial with stepped structure induced multi-resonances," Results in Physics, vol. 18, pp. 1–9, 2020.

[14] C. J. Hodgkinson, D. E. Anagnostou and S. K. Podilchak, "Compact UWB Antipodal Vivaldi Array for Beam Steering Applications," 2021 15th European Conference on Antennas and Propagation (EuCAP), 2021, pp. 1-5.

[15] X. Xiu, W. Che, Y. Han and W. Yang, "Low-Profile Dual-Polarization Frequency-Selective Rasorbers Based on Simple-Structure Lossy Cross-Frame Elements," in IEEE Antennas and Wireless Propagation Letters, vol. 17, no. 6, pp. 1002-1005, June 2018.

[16] Y. Sun, S. Xiao, Z. Yao and Q. Shi, "A Wideband Frequency-Selective Rasorber Based on Interdigital Resonator and Fractal Shaped Slot,"2019 IEEE MTT-S International Wireless Symposium (IWS), 2019, pp. 1-3.

[17] Z. Wang et al., "A High-Transmittance Frequency-Selective Rasorber Based on Dipole Arrays," in IEEE Access, vol. 6, pp. 31367-31374, 2018.

[18] Z. Zhang, Q. Guo and Z. Li, "Frequency Selective Rasorber Based on Tripole Loops and Tripole Slots," 2019 Cross Strait Quad-Regional Radio Science and Wireless Technology Conference (CSQRWC), 2019, pp. 1-3.

[19] Q. Chen, et al., "Design of Absorptive/ Transmissive Frequency-Selective Surface Based on Parallel Resonance," IEEE Transactions on Antennas and Propagation, vol. 65, pp. 4897-4902, 2017.

[20] Q. Chen, et al., "Frequency-Selective Rasorber with Interabsorption Band Transparent Window and Interdigital Resonator," IEEE Transactions on Antennas and Propagation, vol. 66, pp. 4105-4114, 2018.